Measurement Level Integration of Multiple Low-Cost GPS Receivers for UAVs

Akshay Shetty and Grace Xingxin Gao
University of Illinois at Urbana-Champaign

BIOGRAPHY

Akshay Shetty is a graduate student in the Department of Aerospace Engineering, University of Illinois at Urbana-Champaign. He received his B.Tech. in Aerospace Engineering from Indian Institute of Technology Bombay, India in 2014. On graduation, he was awarded the Institute Silver Medal. His research interests include navigation and control of aerospace systems.

Grace Xingxin Gao is an assistant professor in the Aerospace Engineering Department at University of Illinois at Urbana-Champaign. She received her B.S. degree in Mechanical Engineering in 2001 and her M.S. degree in Electrical Engineering in 2003, both at Tsinghua University, China. She obtained her Ph.D. degree in Electrical Engineering at Stanford University in 2008. Before joining Illinois at Urbana-Champaign as an assistant professor in 2012, Prof. Gao was a research associate at Stanford University. Prof. Gao has won a number of awards, including RTCA William E. Jackson Award, Institute of Navigation Early Achievement Award, 50 GNSS Leaders to Watch by GPS World Magazine, and multiple best presentation awards at ION GNSS conferences.

ABSTRACT

UAVs are increasingly being used outdoors for surveillance, exploration, search, rescue and other purposes. A good position estimate allows us to precisely navigate and avoid objects, thus maximising the potential of autonomous applications. There is a growing need for an inexpensive, high performance GPS solution providing better accuracy and robustness. In this paper we incorporate measurements from multiple low-cost, light-weight receivers using an Extended Kalman Filter (EKF). The estimates from the EKF are then compared to the estimates from just one receiver. Experiments are conducted by placing five u-blox receivers on a quadrotor, one on each arm and one at the center. The results show an improvement in accuracy and robustness while using multiple receivers.

INTRODUCTION

Many autonomous tasks depend on the level of accuracy of position estimates given by the respective sensors. In recent times, there has been a sharp increase in the use of Unmanned Aerial Vehicles for outdoor tasks. For such applications, GPS receivers are an easily available option to estimate one's position. However the accuracy of the estimates depends on the quality of the receiver being used, with low-cost GPS receivers providing limited accuracy and robustness. Thus there is a growing demand for a GPS solution providing better accuracy, signal availability and robustness against multipath and other sources of errors.

While integrating the measurements for long durations is an option, it is not suitable for highly dynamical autonomous systems like UAVs. Further, due to the changing orientation of the UAV the antennas face different directions and hence different subsets of the visible satellites. The weight of GPS receivers has to be considered as well. Heavy GPS receivers are not practical for UAVs with limited payload capacity.

Generally, GPS receivers are considered to be black boxes which provide us with position updates. However there are several receivers that allow researchers access to the raw signals as well as the measurements collected by the receivers. There are numerous techniques of using the measurements or raw signals to obtain an improved navigation solution [1,3]. Using an Extended Kalman Filter to incorporate GPS measurements [2] with the Inertial Navigation System is a technique that has been explored in depth [5-8].

The use of multiple low-cost receivers is a field that is gaining importance [3,4]. Different methods of incorporating multiple receivers, like an averaging the latitude-longitude [4] and a raw signal-level integration using Kalman Filter [3], have been previously explored.

The objective of this paper is to propose multiple-receiver architecture with measurement level integration using an Extended Kalman Filter. We proceed to validate this

method by conducting an experiment with multiple low-cost receivers mounted on a UAV.

In the rest of the paper, we will first discuss the algorithm and describe all the matrices being used in the Extended Kalman Filter. We will then look into the experimental setup being used, followed by an analysis of the results.

APPROACH AND ALGORITHM

In this paper, we propose to use multiple low-cost, light-weight receivers from u-blox instead of just one. We place one receiver on each arm of a quadrotor and another one at the center. We then carry out a measurement level integration of all the receivers to obtain a better estimate for the position of the center of the quadrotor. An Extended Kalman Filter is used for integrating the measurements and estimating the states, which includes the position of the quadrotor. Since the frame of the quadrotor is rigid and the GPS receivers are fixed on it, the position and dynamics of the receivers are related to each other and hence constrained.

Figure 1 shows a simple block diagram for the multi-receiver architecture.

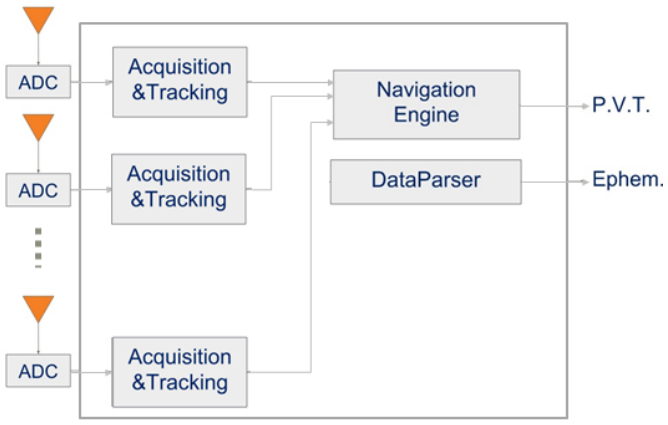

Figure 1. Approach overview. Multiple antennas track the signals from visible GPS satellites. These signals are sent to the respective receivers. Each receiver then applies acquisition and tracking algorithms to generate measurements like the pseudorange and the carrier phase. Finally the pseudorange measurements from all the receivers are then used in an extended Kalman filter, which estimates the position of the quadrotor.

The following is the state vector being used in the EKF:

x	$ECEF\ x\ coordinate$
y	$ECEF\ y\ coordinate$
z	$ECEF\ z\ coordinate$
$\dot{x}$	$ECEF\ x\ velocity$
$\dot{y}$	$ECEF\ y\ velocity$
$\dot{z}$	$ECEF\ z\ velocity$
ϕ	$Roll$
θ	$Pitch$
ψ	Yaw
$\dot{\phi}$	$Roll\ rate$
$\dot{\theta}$	$Pitch\ rate$
$\dot{\psi}$	$Yaw\ rate$
$c\delta t_1$	$Receiver\ 1\ clock\ bias$
$c\dot{\delta} t_1$	$Receiver\ 1\ clock\ bias\ rate$
$c\delta t_2$	$Receiver\ 2\ clock\ bias$
$c\dot{\delta} t_2$	$Receiver\ 2\ clock\ bias\ rate$
$c\delta t_3$	$Receiver\ 3\ clock\ bias$
$c\dot{\delta} t_3$	$Receiver\ 3\ clock\ bias\ rate$
$c\delta t_4$	$Receiver\ 4\ clock\ bias$
$c\dot{\delta} t_4$	$Receiver\ 4\ clock\ bias\ rate$
$c\delta t_5$	$Receiver\ 5\ clock\ bias$
$c\dot{\delta} t_5$	$Receiver\ 5\ clock\ bias\ rate$

Here ECEF refers to the Earth-Centered, Earth-Fixed Cartesian corordinate system.

Though we are currently estimating only the position, the velocities and attitude rates are included to easily incorporate the carrier phase measurements at a later stage. The dynamic model currently used, is a constant velocity model. The state transition matrix can be separated into three independent parts: the position states, the attitude states and the clock bias states. The position and attitude state transition matrices can be written as:

$$\Phi_{xyz} = \Phi_{\phi\theta\psi} = \begin{bmatrix} 1 & 0 & 0 & \Delta t & 0 & 0 \\ 0 & 1 & 0 & 0 & \Delta t & 0 \\ 0 & 0 & 1 & 0 & 0 & \Delta t \\ 0 & 0 & 0 & 1 & 0 & 0 \\ 0 & 0 & 0 & 0 & 1 & 0 \\ 0 & 0 & 0 & 0 & 0 & 1 \end{bmatrix}$$

The state transition matrix for each clock bias can be represented as:

$$\Phi_{c\delta t_i} = \begin{bmatrix} 1 & \Delta t \\ 0 & 1 \end{bmatrix}$$

Where *i* varies from 1 to 5.

Finally, combining all three, we get the complete state transition matrix:

$$\Phi = \begin{bmatrix} \Phi_{xyz} & 0 & 0 & 0 & 0 & 0 & 0 \\ 0 & \Phi_{\phi\theta\psi} & 0 & 0 & 0 & 0 & 0 \\ 0 & 0 & \Phi_{c\delta t_1} & 0 & 0 & 0 & 0 \\ 0 & 0 & 0 & \Phi_{c\delta t_2} & 0 & 0 & 0 \\ 0 & 0 & 0 & 0 & \Phi_{c\delta t_3} & 0 & 0 \\ 0 & 0 & 0 & 0 & 0 & \Phi_{c\delta t_4} & 0 \\ 0 & 0 & 0 & 0 & 0 & 0 & \Phi_{c\delta t_5} \end{bmatrix}$$

The next task is to relate the measurements to the states. We can write the corrected pseudorange measurement from the k[th] satellite, simply as:

$$\rho_c^{(k)} = ||\boldsymbol{x}^{(k)} - \boldsymbol{x}|| + c.\,\delta t_u + \tilde{\varepsilon}_\rho^{(k)}$$

Where: $||\boldsymbol{x}^{(k)} - \boldsymbol{x}||$ is the actual distance between the receiver antenna and the k[th] satellite.

δt_u, is the receiver clock bias.

$\tilde{\varepsilon}_\rho^{(k)}$, accounts for modeling errors and unmodeled effects.

Therefore, a row in the observation matrix will be the partial derivative of the above equation with respect to the states. For example, a pseudorange measurement from the center receiver can be written as follows:

$$H_1^{(k)} = \left[\left(-1^{(k)}\right)^T \; 0\;0\;0\;0\;0\;0\;0\;0\;0\cdots \right.$$
$$\left. \cdots 1\;0\;0\;0\;0\;0\;0\;0\;0\;0\right]$$

Where: $H_1^{(k)}$ represents the pseudorange measurement between the k[th] satellite and the 1[st] receiver.

$(-1^{(k)})$ is a vector with direction cosines drawn from receiver position to the k[th] satellite.

For receivers which are on the quadrotor arms, their position relative to the center is known in the body frame. This relative vector is rotated to the ECEF frame using two rotation matrices. The first rotation matrix transforms the vector to the local East-North-Up frame (ENU). This matrix depends on the attitude of the quadrotor. The second rotation matrix transforms the vector to the ECEF frame. This matrix depends on the latitude and longitude of the quadrotor. These angles are obtained using the previous state estimates and the World Geodetic System 1984 (WGS 84).

The complete observation matrix can be written as:

$$H = \begin{bmatrix} H_1^{(1)} \\ \vdots \\ H_1^{(n_1)} \\ H_2^{(1)} \\ \vdots \\ H_2^{(n_2)} \\ H_3^{(1)} \\ \vdots \\ H_3^{(n_3)} \\ H_4^{(1)} \\ \vdots \\ H_4^{(n_4)} \\ H_5^{(1)} \\ \vdots \\ H_5^{(n_5)} \end{bmatrix}, \begin{matrix} n_i\text{: no. of satellites} \\ \text{seen by } i^{th} \text{ receiver} \end{matrix}$$

The process and observation noises are both chosen to be zero mean multivariate Gaussian noises with covariance Q and R. Process noise covariance for the position states:

$$Q_{xyz} = \begin{bmatrix} S_P\frac{\Delta t^3}{3} & 0 & 0 & S_P\frac{\Delta t^2}{2} & 0 & 0 \\ 0 & S_P\frac{\Delta t^3}{3} & 0 & 0 & S_P\frac{\Delta t^2}{2} & 0 \\ 0 & 0 & S_P\frac{\Delta t^3}{3} & 0 & 0 & S_P\frac{\Delta t^2}{2} \\ S_P\frac{\Delta t^2}{2} & 0 & 0 & S_P\Delta t & 0 & 0 \\ 0 & S_P\frac{\Delta t^2}{2} & 0 & 0 & S_P\Delta t & 0 \\ 0 & 0 & S_P\frac{\Delta t^2}{2} & 0 & 0 & S_P\Delta t \end{bmatrix}$$

The covariance matrix for the attitude states is similar and can be written as:

$$Q_{\phi\theta\psi} = \begin{bmatrix} S_A\frac{\Delta t^3}{3} & 0 & 0 & S_A\frac{\Delta t^2}{2} & 0 & 0 \\ 0 & S_A\frac{\Delta t^3}{3} & 0 & 0 & S_A\frac{\Delta t^2}{2} & 0 \\ 0 & 0 & S_A\frac{\Delta t^3}{3} & 0 & 0 & S_A\frac{\Delta t^2}{2} \\ S_A\frac{\Delta t^2}{2} & 0 & 0 & S_A\Delta t & 0 & 0 \\ 0 & S_A\frac{\Delta t^2}{2} & 0 & 0 & S_A\Delta t & 0 \\ 0 & 0 & S_A\frac{\Delta t^2}{2} & 0 & 0 & S_A\Delta t \end{bmatrix}$$

The covariance matrix used for the clock biases is:

$$Q_{c\delta t_i} = \begin{bmatrix} S_f \Delta t + S_g \frac{\Delta t^3}{3} & S_g \frac{\Delta t^2}{2} \\ S_g \frac{\Delta t^2}{2} & S_g \Delta t \end{bmatrix}$$

Thus, the complete process noise covariance matrix looks like:

$$Q = \begin{bmatrix} Q_{xyz} & 0 & 0 & 0 & 0 & 0 & 0 \\ 0 & Q_{\phi\theta\psi} & 0 & 0 & 0 & 0 & 0 \\ 0 & 0 & Q_{c\delta t_1} & 0 & 0 & 0 & 0 \\ 0 & 0 & 0 & Q_{c\delta t_2} & 0 & 0 & 0 \\ 0 & 0 & 0 & 0 & Q_{c\delta t_3} & 0 & 0 \\ 0 & 0 & 0 & 0 & 0 & Q_{c\delta t_4} & 0 \\ 0 & 0 & 0 & 0 & 0 & 0 & Q_{c\delta t_5} \end{bmatrix}$$

The values of S_P, S_A and S_g are chosen depending on the accuracy of the model. A detailed derivation of the matrices can be found in [2].

The measurement noise covariance matrix R, is taken to be a diagonal matrix as shown below:

$$R = \begin{bmatrix} r_\rho & 0 & \cdots & 0 \\ 0 & r_\rho & \ddots & \vdots \\ \vdots & \ddots & \ddots & 0 \\ 0 & \cdots & 0 & r_\rho \end{bmatrix}$$

Here R is a square matrix, of size equal to the number of available measurements. With the above matrices ready, we then use the standard discrete-time predict and update equations:

Predict

Predicted state estimate:

$$\hat{\boldsymbol{x}}_{k|k-1} = f(\hat{\boldsymbol{x}}_{k-1|k-1}, \boldsymbol{u}_{k-1})$$

Predicted covariance estimate:

$$\boldsymbol{P}_{k|k-1} = \boldsymbol{\Phi}_{k-1} \boldsymbol{P}_{k-1|k-1} \boldsymbol{\Phi}_{k-1}^T + \boldsymbol{Q}_{k-1}$$

Update

Measurement Residual:

$$\tilde{\boldsymbol{y}}_k = \boldsymbol{z}_k - h(\hat{\boldsymbol{x}}_{k|k-1})$$

Residual Covariance:

$$\boldsymbol{S}_k = \boldsymbol{H}_k \boldsymbol{P}_{k|k-1} \boldsymbol{H}_k^T + \boldsymbol{R}_k$$

Near-optimal Kalman Gain:

$$\boldsymbol{K}_k = \boldsymbol{P}_{k|k-1} \boldsymbol{H}_k^T \boldsymbol{S}_k^{-1}$$

Updated state estimate:

$$\hat{\boldsymbol{x}}_{k|k} = \hat{\boldsymbol{x}}_{k|k-1} + \boldsymbol{K}_k \tilde{\boldsymbol{y}}_k$$

Updated covariance estimate:

$$\boldsymbol{P}_{k|k} = (\boldsymbol{I} - \boldsymbol{K}_k \boldsymbol{H}_k) \boldsymbol{P}_{k|k-1}$$

Where the state transition and observation matrices are defined to be the following Jacobians:

$$\boldsymbol{F}_{k-1} = \left. \frac{\partial f}{\partial \boldsymbol{x}} \right|_{\hat{\boldsymbol{x}}_{k-1|k-1}, \boldsymbol{u}_{k-1}}$$

$$\boldsymbol{H}_k = \left. \frac{\partial h}{\partial \boldsymbol{x}} \right|_{\hat{\boldsymbol{x}}_{k|k-1}}$$

EXPERIMENTAL SETUP

To implement this approach, we use the Pelican quadrotor manufactured by Ascending Technologies. The Pelican offers plenty of space and various interfaces for individual components and payloads. This top quality and safe aerial robot is a highly reliable platform for research purposes.

For our experiment, we need to record messages from five u-blox receivers simultaneously. In order to log these messages we use an onboard computer, the AscTec Mastermind. The AscTec Mastermind, preinstalled with a Linux OS, has a high performing 3rd Generation Intel® Core™ i7 processor. Further, it has multiple USB ports which allow us to connect five u-blox receivers simultaneously.

The processor on the Pelican has two levels: Low Level Processor (LLP) and High Level Processor (HLP). The LLP has pre-installed codes for attitude and position control and it also receives the IMU readings. The HLP interacts with the LLP and allows the user to define his own programs in C using the AscTec Software Development Kit (available online). The communication between the Mastermind and HLP is carried out with the help of AscTec Communication Interface, a new method of communication between the device and the local machine.

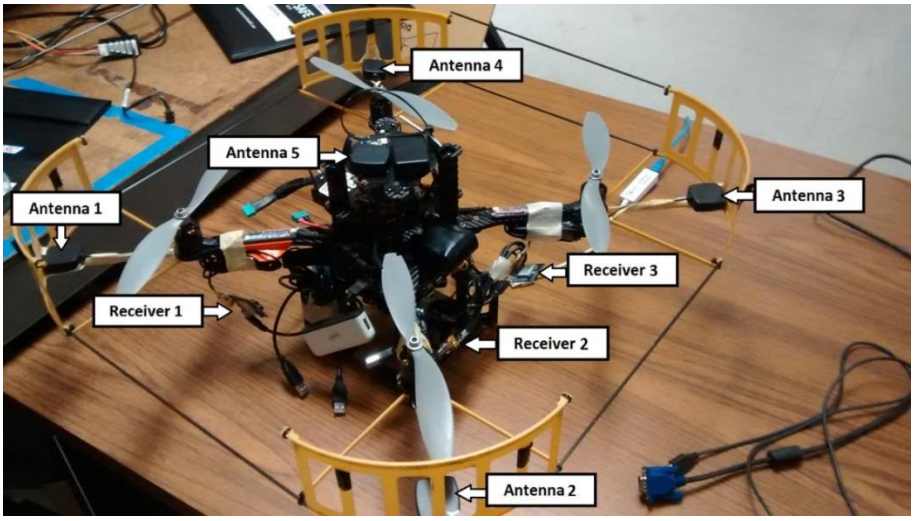

Figure 2. The AscTec Pelican labelled with the visible u-blox receivers and antennae placed on it. There is one receiver on each arm of the Pelican, and one at the center.

To read the required messages from the u-blox receivers we run a Python code on the Mastermind. Our code requests the u-blox receiver to send the required data, and writes the measurements with a frequency of 1 Hz into text files for further use. As shown in Figure 2, there is one antenna at the center of the Pelican, and one on the end of each arm.
For collecting the data, we took the Pelican to the roof of our Talbot Laboratory. We kept it stationary for about 25 minutes to ensure that the entire ephemeris data was downloaded. After that the Pelican was moved from the South-East corner to the North-West corner, and then back.

Using the text files from the Mastermind, we then implement the Extended Kalman Filter to obtain estimates for the position of the Pelican. The estimates from the multiple-receiver case are compared to the estimates from using the center receiver only.

RESULTS

The Pelican was initially kept stationary and the position estimates from the multiple-receivers and the center receiver are compared. Figure 3 shows the variations in estimated ECEF co-ordinates. The estimates are offset by their mean value to have a good comparison of the variations.

We see an improvement in the standard deviations. Using only the center receiver we obtain a standard deviation of 2.4896 meters, while using all the five receivers gives us a standard deviation of 0.9207 meters.

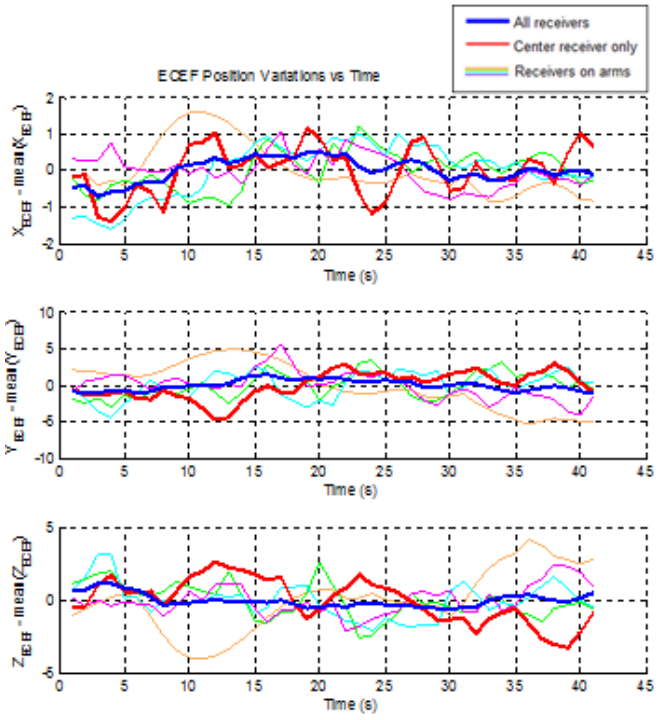

Figure 3. Variations in the position estimates of the stationary Pelican. The standard deviations using multiple-receivers are: [0.3227 0.7333 0.4536] meters in the ECEF x, y and z co-ordinates respectively. Using only the center receiver, we get standard deviations: [0.6780 1.8482 1.5240] meters.

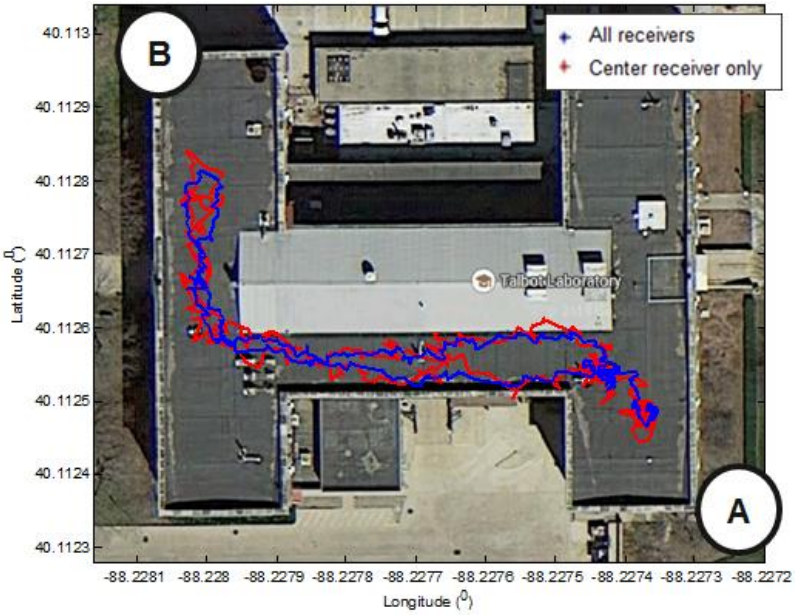

Figure 5. 2D trajectory of the Pelican on the Talbot Lab roof. It was moved from Point A to Point B, and then back to Point A. The multiple-receiver solution looks more accurate and is less scattered compared to the solution from the center receiver only.

With time, the visible set of satellites keeps changing. When a receiver stops tracking a satellite, the number of equations in the measurement matrix changes and there is a jump in the estimates. Figure 4 shows the improvement in robustness while using multiple receivers. The variations are plotted for when the center receiver stops tracking satellite ID 16. There is a sharp jump observed in the estimates from the center receiver while the estimates from the multiple receivers also deviate, but to a much smaller extent.

There is a small deviation observed in the multiple satellite solution when one of the receivers loses a satellite from view. Since there are five receivers being used, the probability of one of the receivers losing a satellite is higher. Hence, though the multiple-receiver solution is more robust, it might have a higher number of such small deviations.

Figure 5 shows a 2D plot of the trajectory the Pelican was moved along, on the roof of Talbot Laboratory. The Pelican was kept in the South-East corner at point A and then moved to the North-West corner at point B, and then taken back to A again.

In the figure we can see that the solution from the center receiver (red points) has more stray points compared to the solution from multiple receivers (blue points).

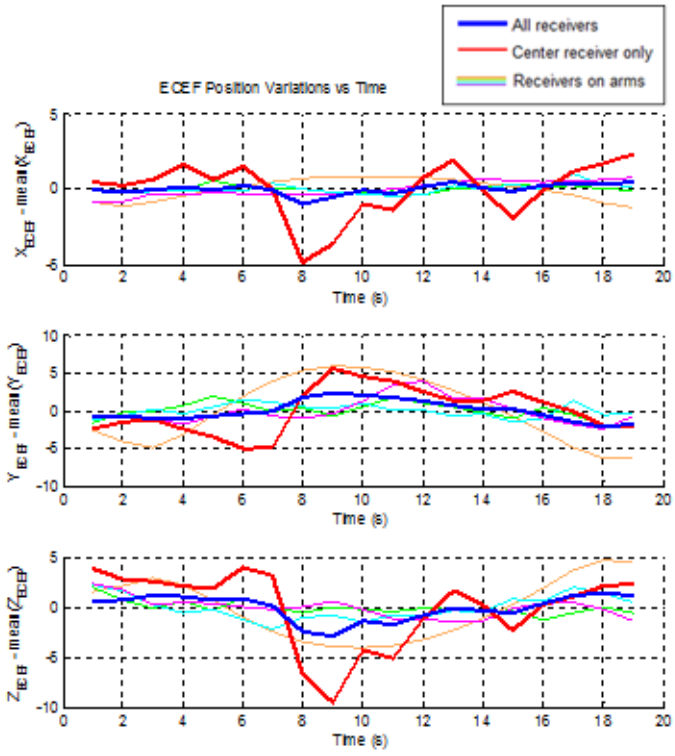

Figure 4. Variation in the position estimates while losing satellite ID 16 from view. There is a sharp jump in the estimates using only the center receiver, but the multiple-receiver solution is more robust to such a change.

CONCLUSION

In this paper, we have proposed multiple-receiver architecture with measurement level integration for unmanned aerial vehicles. We implemented an Extended Kalman Filter for the purpose of integrating the pseudorange measurements from multiple receivers.

The measurement matrix in the EKF can be further extended to include the carrier phase measurements from the receivers. This can help us in estimating the attitude of the quadrotor. Furthermore, the measurement noise covariance matrices can be altered to give weightages to different receivers. The weights can be assigned based on various metrics like the signal-to-noise ratio or the elevation angles.

To validate the approach discussed in this paper, we placed five u-blox receivers on the Pelican and stored their messages in the Mastermind. Experiments were conducted by moving the Pelican on the roof of Talbot Laboratory. On comparing the solutions from multiple-receivers and from the center receiver only, we demonstrated an improvement in the accuracy and the robustness.

REFERENCES

[1] P. Misra and P. Enge, *Global Positioning System: Signals, Measurements, and Performance*, Revised 2nd ed. Lincoln, MA: Ganga-Jamuna Press, 2012.

[2] R. G. Brown and P. Y. C. Hwang, *Introduction to Random Signals and Applied Kalman Filtering*, 3rd ed. John Wiley and Sons, Inc., 1997.

[3] A. Soloviev, J. Dickman, J. Campbell, "Collaborative GNSS Receiver Architecture for Weak Signal Processing" in *Proceedings of International Technical Meeting (ITM) of The Institute of Navigation San Diego, CA, January 28-30, 2013.*

[4] D. Schrader, B.-C. Min, E. Matson, and J. Dietz, "Combining multiple, inexpensive GPS receivers to improve accuracy and reliability," in Sensors Applications Symposium (SAS), 2012 IEEE, Feb. 2012, pp.1-6.

[5] J. Ryu and J. C. Gerdes, "Integrating inertial sensors with global positioning system (gps) for vehicle dynamics control," Journal of Dynamic Systems, Measurement, and Control, vol. 126, no. 2, pp. 243–254, 2004.

[6] S. Godha and M. E. Cannon, "GPS/MEMS INS integrated system for navigation in urban areas," GPS Solutions, vol. 11, pp. 193–203, Jan. 2007.

[7] Da, Ren, Dedes, George, Shubert, Keith, "Design and Analysis of a High-Accuracy Airborne GPS/INS System," *Proceedings of the 9th International Technical Meeting of the Satellite Division of The Institute of Navigation (ION GPS 1996)*, Kansas City, MO, September 1996, pp. 955-964.

[8] Masson, A., Burtin, D., Sebe, M., "KINEMATIC DGPS AND INS HYBRIDIZATION FOR PRECISE TRAJECTORY DETERMINATION", *NAVIGATION, Journal of The Institute of Navigation*, Vol. 44, No. 3, Fall 1997, pp. 313-322.